Chapter 4
Results and Discussion

4.1 Results

4.1.1 Introduction

The emissions results for the each test are presented in this chapter. The results are presented in graph and table form. The results displayed include HC, CO emission levels, and the number of cycles after fuel is supplied until the engine starts. The measured concentrations of HC ,CO are presented against time elapsed. Time elapsed starts after the first successful engine fire. Plots showing the results for NO_x, CO_2, and O_2 emissions are provided in the appendix. They were not included in this section, because they do not show any changes outside of those induced through the variation in test conditions.

While plots of concentration versus time were used to present HC emissions, two additional presentation methods were used for the HC emissions data. The first alternative method has the measured HC concentration normalized against the HC concentration measured 120 seconds after the engine's start (Equation 4.1).

$$HC_{norm}(t) = \frac{HC(t)}{HC(120\,\text{sec.})} \qquad \text{Eq. 4.1}$$

The normalized value is graphed versus time. The HC concentration at 120 seconds was considered the HC concentration produced when the engine was full warmed up, because after 120 seconds the level stayed relatively flat. The average time required for automotive catalyst to reach operation temperature is also around 2 minutes. At this point the catalyst completes incomplete combustion. The post 120 seconds HC emission showed slight fluctuation due to slight unforeseen fluctuations in volumetric efficiency induced by the cooling method.

The second alternative method in which the HC emissions are presented shows the percent increase in the mass of HC emissions over the first 120 seconds of a cold start when compared to the mass of the engine's warmed HC emissions over a 120 second period (Equation 4.2). This produced a single value which was plotted against number of cycles to start data for the corresponding run at the appropriate ignition energy.

$$\%Increase_{HC} = \frac{\int_0^{120} HCdt - HC_{120\sec}(120)}{HC_{120\sec}(120)} \times 100 \qquad \text{Eq. 4.2}$$

4.1.2 Hydrocarbon Emissions

The effect of increased ignition energy on Cold Start HC emissions was the focus of the study. The emissions measured for the three increasing ignition energy levels (stock, +0.387 J, +1.187 J) are presented in Figures 4.1.-4.10. Figures 4.1, 4.3, 4.5 display the recorded HC emissions versus time after initial startup. Normalized HC emissions versus time are presented in Figures 4.2, 4.4, 4.6.

HC emissions for the stock ignition are presented in Figures 4.1, 4.2. The recorded HC concentration data over the first 120 seconds of each run shows the peak HC emissions for each experimental run occurring in the first 15 seconds. The peak HC emission levels for the stock ignition energy exhibit a fair amount of variation. The peak HC concentrations for the stock ignition energy range from 3.5 to 8.5 times the HC level produced by the engine once it was warmed. The normalized graph displays the variation best (Figure 4.2). Table 4.1 lists the actual peak HC levels for each run.

Table 4.1 - Cold Start Hydrocarbon Emissions Peak Level Comparison for Runs With Stock Ignition Energy

Run #	Peak HC (PPM)	# Cycles Until Start			
1	730	10	Average =	860	
2	838	11	Std Deviation (samp) =	163	
3	1200	15			
6	859	9			
7	944	12		Upper Bound	Lower Bound
8	817	10	Confidence Interval (95%) =	740	980
9	841	9	Confidence Interval (99%) =	675	1045
10	650	9			

Table 4.1. also shows the standard deviation of the sample and the confidence interval calculated from the student-t distribution method.

The second set of data shows the HC emissions when the additional 0.387 joules of ignition energy were added to the stock ignition system's output (Figures 4.4, 4.6). The HC emissions resulting from the 0.387 joules increase in the ignition energy are similar to the performance of the stock ignitions system. The HC peak emissions demonstrate similar amounts of scatter ranging from 4 to 7 times the concentration of HC emitted when the engine was warm. One run at 0.387 joules additional ignition energy had a HC peak 11 times that warmed HC concentration level. This run seems out of the reasonable range of the expected HC concentrations. Removing this run shifts the peak HC average from 880 to 817 ppm. Table 4.2 lists the peak cold start HC concentrations for the additional 0.387 joules of energy over the stock ignition energy levels. The data shows no significant increase in performance between stock and the additional 0.387 joules. If the one extreme run is omitted it could be argued that there is a minimal decrease in HC emission but the random nature of the cold start process supports leaving the run in the sample population.

Table 4.2 - Cold Start Hydrocarbon Emissions Peak Level Comparison for Runs With 0.387 Joules of Additional Ignition Energy

Run #	Peak HC (PPM)	# Cycles Until Start			
1	1028	10	Average =	880	
2	1441	19	Std Deviation (samp) =	229	
3	687	10			
4	753	7			
5	804	12		Upper Bound	Lower Bound
6	800	8	Confidence Interval (95%) =	740	1020
7	1016	14	Confidence Interval (99%) =	664	1095
8	719	9			
9	725	8			
10	824	8			

The cold start HC emissions resulting from the addition of 1.185 joules of energy to the stock ignition systems show slight improvements over the stock ignition and the 0.387 joule increase over stock. Figures 4.5 and 4.6 show the HC emissions for 1.185 joules of additional energy versus time. Peak HC concentrations during the cold start for the 1.187 joule runs takes place within the first 15 seconds. This trend is similar to the stock ignition and 0.387 joule runs. Unlike the test runs performed at lower ignition energy, the peak HC level is lower. The variation in the peak HC concentration values is less. Table 4.3 lists the values of the peak HC emissions, the standard deviation, and the confidence interval.

Table 4.3 - Cold Start Hydrocarbon Emissions Peak Level Comparison for Runs With 1.187 Joules Additional Energy

Run #	Peak HC (PPM)	# Cycles Until Start			
1	672	8	Average =	739	
2	740	9	Std Deviation (samp) =	70	
3	659	8			
4	779	10			
5	727	8		Upper Bound	Lower Bound
6	869	9	Confidence Interval (95%) =	664	814
7	728	10	Confidence Interval (99%) =	607	871

Figure 4.7 summarizes the HC emissions for the three energy levels. For the three ignition energy levels, the percent increase in the level of HC emission production in the first 120 seconds due to the cold start over the level of HC production by the engine, fully warmed, in an 120 second period is plotted for each run. On the graph, the test runs for the stock ignition and the 0.387 joules additional energy runs exhibit similar behavior. Both stock and 0.387 joules runs exhibit large amounts of scatter in the percent increase in HC production. The runs at 1.187 joules of additional energy have less scatter and average a lower HC emissions level. In Figure 4.8, the percent increase in cold start HC emissions is plotted versus the number of cycles before the engine starts after first amount of fuel was injected. On this graph and Figure 4.9, the same level of scatter exhibited on the % increase in HC emissions and cycles to start can be seen. Once again, the 1.187 joules additional energy data points have less variance

The amount of HC emissions in general increases as the number of cycles to start increases. The highest peak levels of HC's emitted for each ignition energy level

occurred on the test runs were the engine required an increased number of initial cycles to fire
(Table 4.1-4.3). With each cycle that does not sustaining combustion, a substantial portion of the fuel being injected is pass through to the exhaust. Large increases in the number of cycles until start should result in an increase in HC emission given that the amount of fuel supplied is equal in a cases. The 1.187 joule additional energy setting experienced small changes in number of cycles (within the 2 cycle of uncertainty) until start. The effects of these small changes in cycles to start on the HC emission are not as pronounced. The constantly low cycles until start do correlate to lower HC emissions for the 1.187 joule energy level.

4.1.3 Carbon Monoxide Emissions

The Carbon Monoxide emissions data for the three ignition energy levels over the first 120 seconds are presented in Figures 4.9 - 4.11. The CO emissions graphs for all 3 ignition energy levels have similar trends. The graphs show a initial rise in CO concentration to around 0.23 %. The CO level then decreases to around 0.19% by the 40 second mark. The difference in the level of CO in the initial rise for stock ignition energy and the additional 0.387 is between .01% and 0.02%. These values fall within the uncertainty of the CO analyzer's measurement. The stock ignition system produces CO concentration peaks that range from .24% to . 34% The majority of the population is between 0.24 % and 0.25%. The two runs of the stock ignition that exhibit high CO concentration peaks are runs that had low levels of HC emissions. The levels for those two runs was comparable to the runs performed at 1.187 joules of additional energy. The two runs could have experienced optimum air/fuel mixtures at the plug. The CO concentration for the 0.387 joules of additional energy peaked between 0.23% and 0.26%. The variation in CO was lower for this run. When 1.187 joules of energy was added to the stock ignition, CO levels increased for majority of the runs. The increased amounts of HC oxidized created the slight increase in the initial CO levels for the 1.187 joules additional energy runs. The level of CO produced at 1.187 joules of addition energy vary from 0.32% to .24%. The ranges of CO concentrations overlapped for the three energy levels.

After the first 50 seconds the CO levels rise again (Figure 4.11-4.13). Unexpected variations in air/fuel ratio cause for the rise and fall behavior exhibited by the CO emission. The variation is induced by changes in fuel injector opening pulse function with time coupled with unaccounted for changes in volumetric efficiency. The discussion section covers the trend in more detail. The effect was constant through out all test runs so it is not suspected to have interfered with credibility of the test.

4.1.4 Number Of Cycles Until the First Successful Fire

Figure 4.9 shows the range in the number of cycles counted until the first successful fire was sensed after the fueling sequence was initiated. Figure 4.8 and Tables 4.1-4.3 similar data relating cycle to start data to HC emissions. The stock ignition system recorded starts within 9 to 15 cycles after being supplied with fuel. The engine operating at 900 RPM or 15 Hz, translates into 7.5 combustion cycles per second for a 4 stroke engine. Operating at this constant, speed the engine started within 1.2 to 2 seconds after fuel was supplied. The second energy ignition energy level, 0.387 joules over stock ignition energy, also displayed a large spread in the number of cycles until start. The number of cycles until start for the 0.387 joules over stock ignition energy runs varied from 7 to 14 with one run starting in 19 cycles. The time until start ranged .93 to 1.87 seconds and 2.53 seconds respectively. The slight increase in ignition energy (+0.387 J) showed no performance increase in the number of cycle to start data. The data for experimental runs at 1.187 joules over stock ignition energy demonstrated less spread in the number of cycles until start. The number of cycles until start range form 8 to 10 or 1.06 seconds to 1.33 seconds. In Figure 4.9, some of the data points lye on top of one another but their distribution is better displayed in Figure 4.8. Error bars in figure 4.8 are set at 2 cycles based on estimated reaction time between hearing engine start and triggering counter.

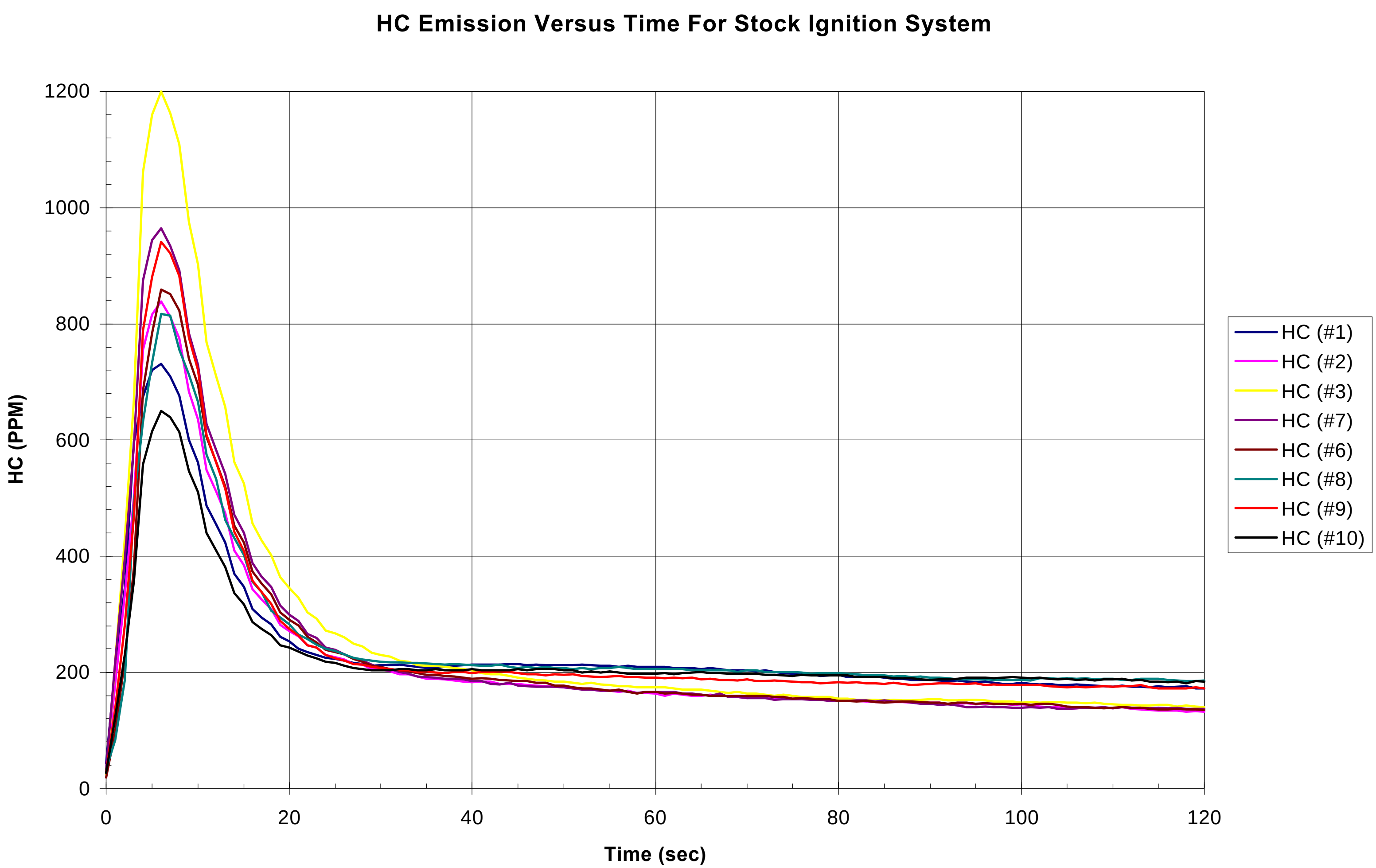

Figure 4.1 - HC Emissions For Stock Ignition System

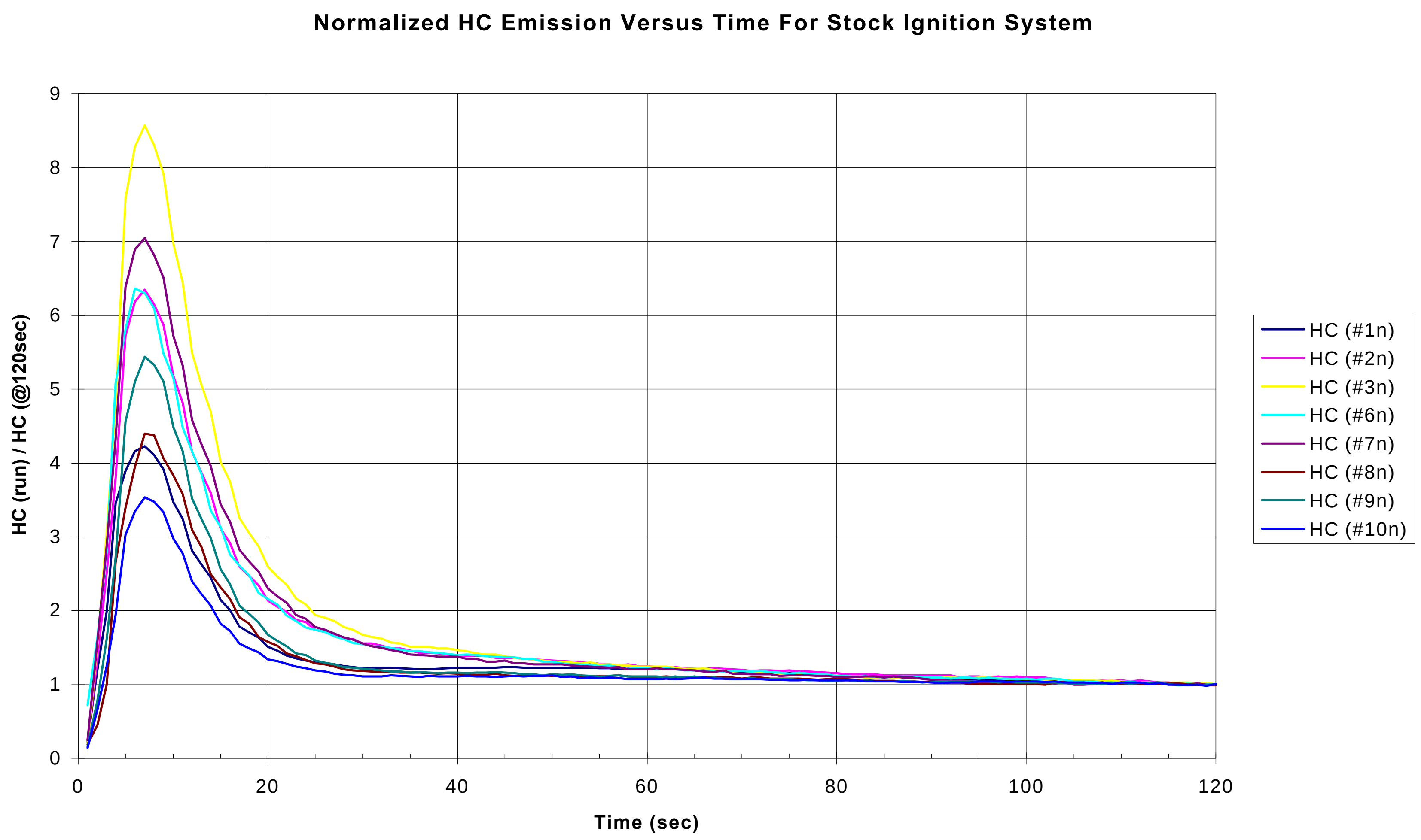

Figure 4.2 - Normalized HC Emissions For Stock Ignition System

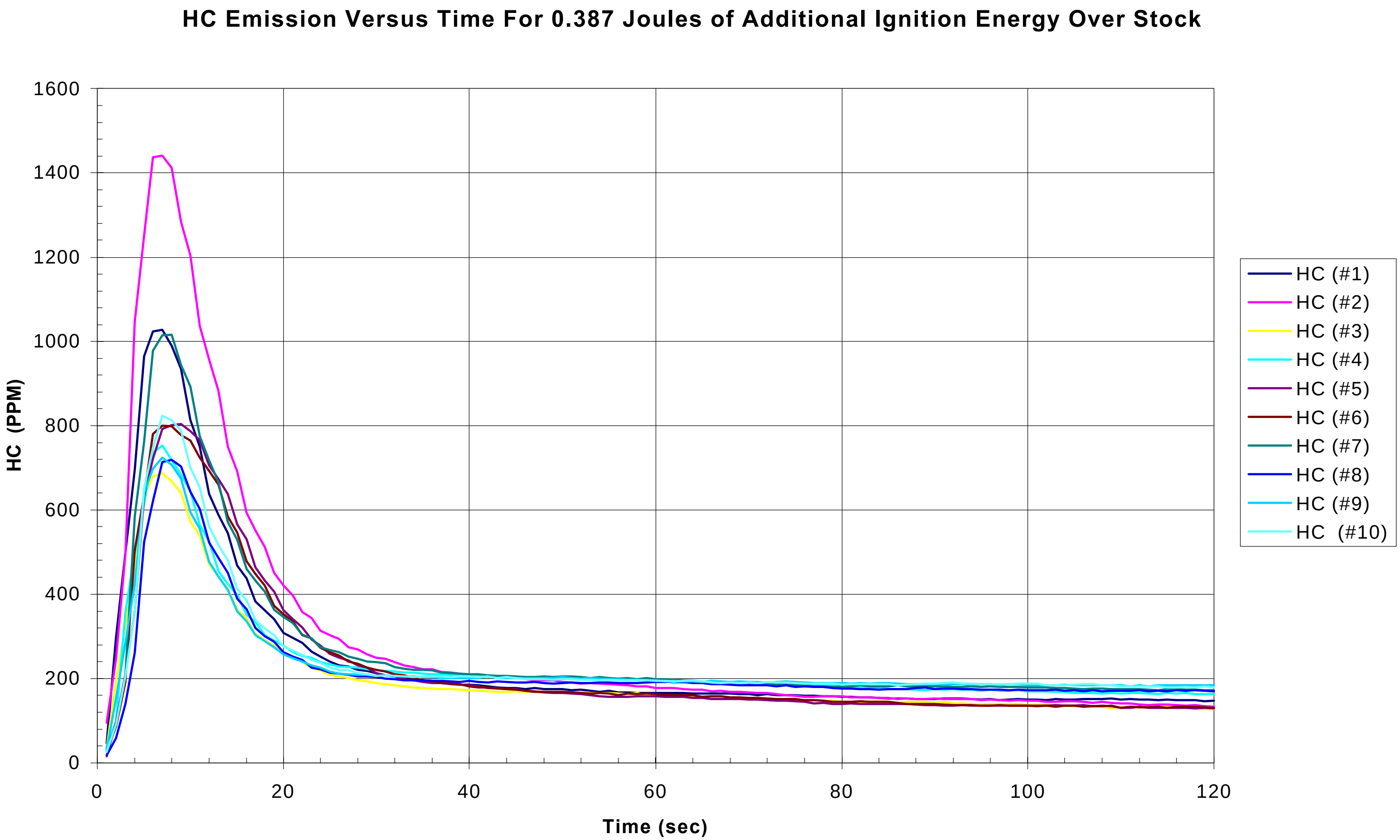

Figure 4.3 - HC Emissions For 0.387 Joules of Additional Energy Over Stock

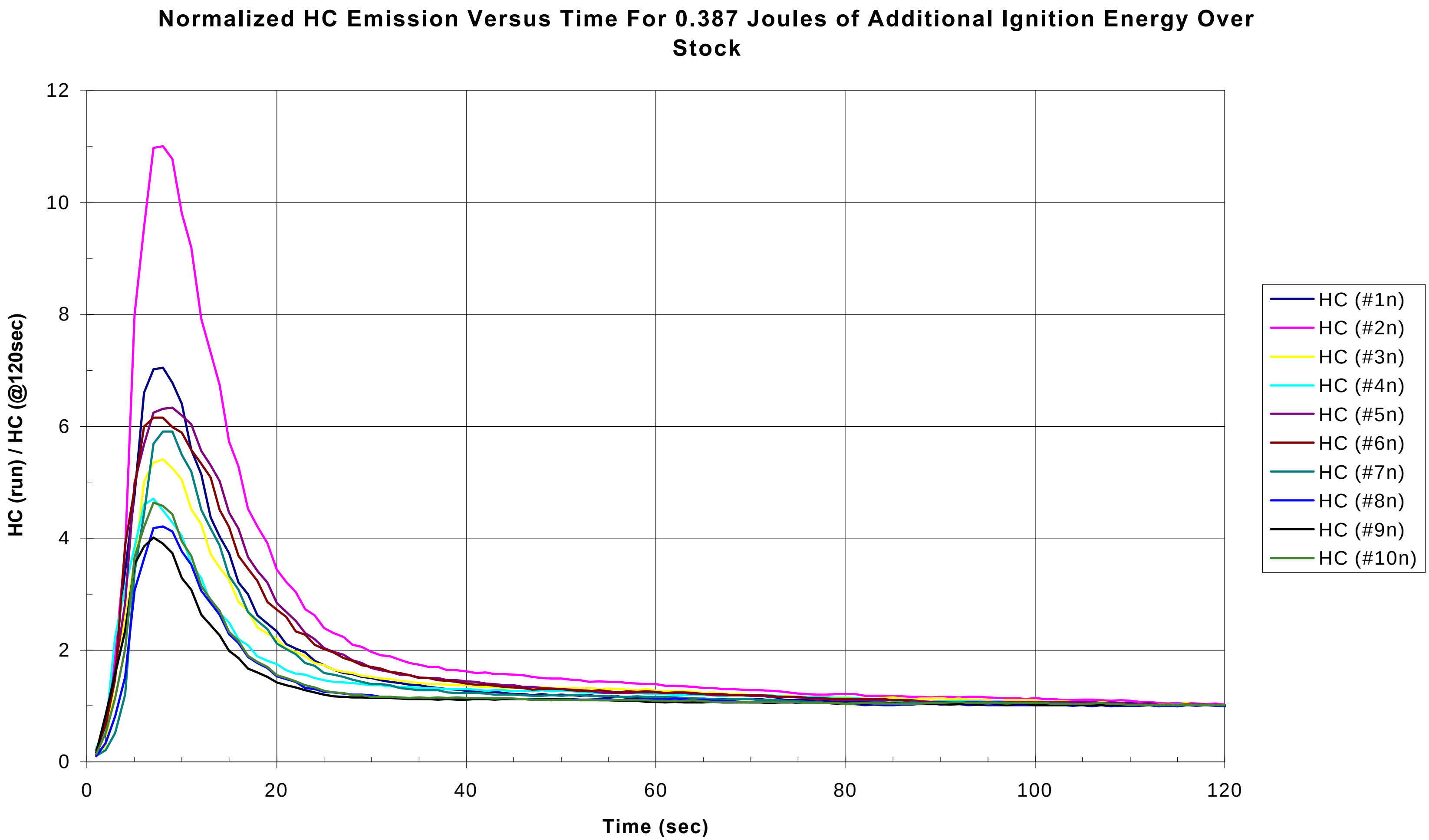

Figure 4.4 - Normalized HC Emissions For 0.387 Joules of Additional Energy Over Stock

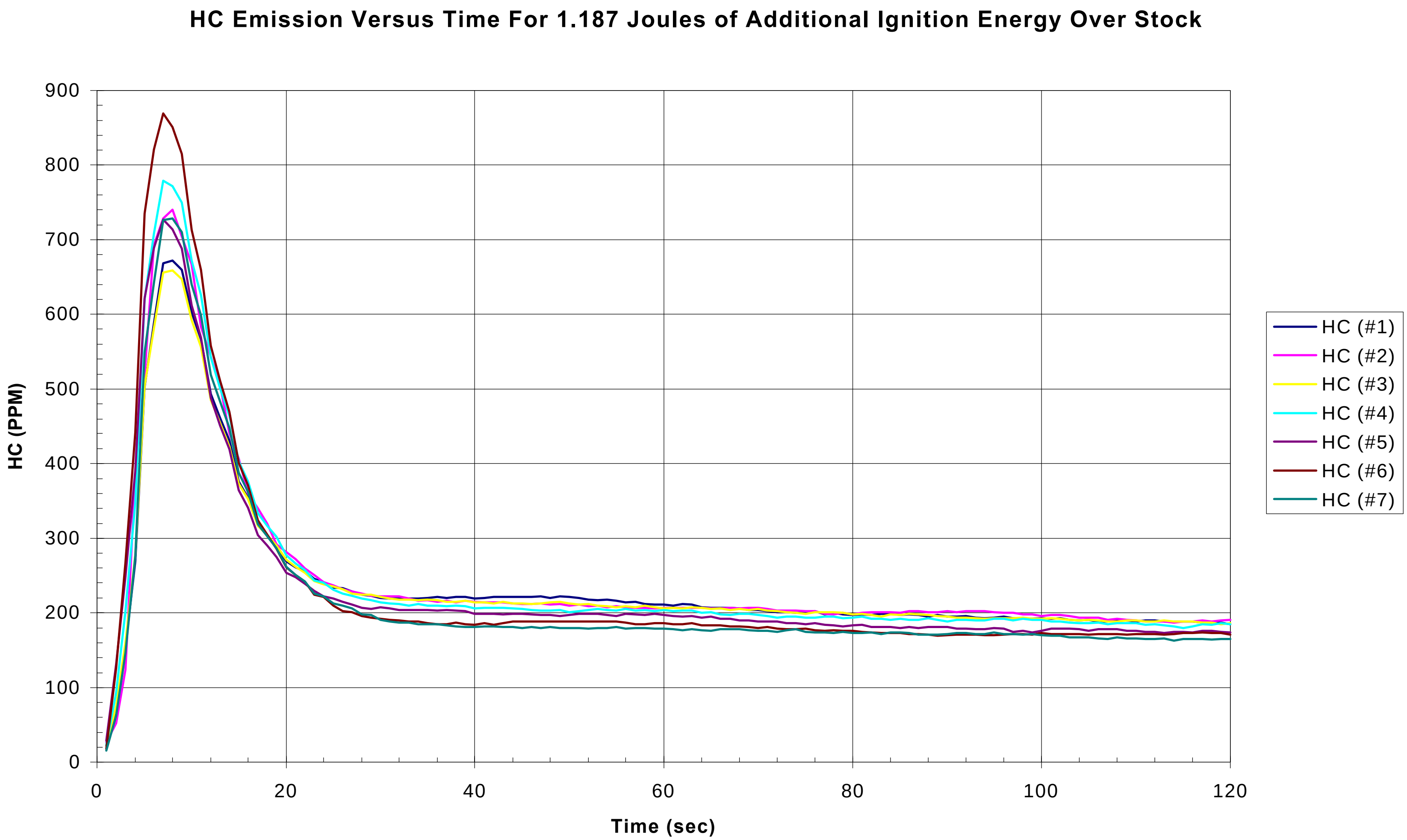

Figure 4.5 - HC Emissions For 1.187 Joules of Additional Energy Over Stock

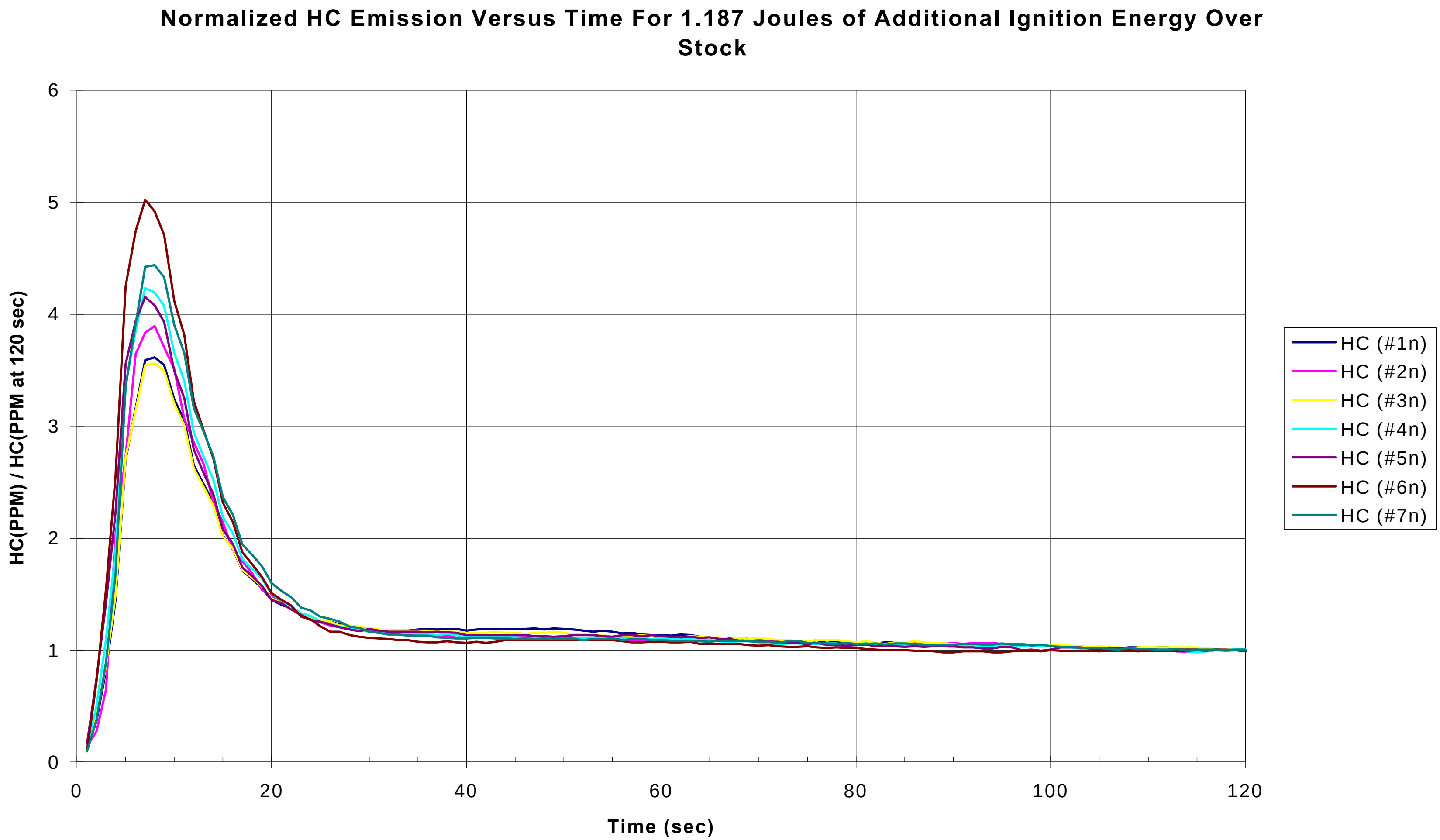

Figure 4.6 - Normalized HC Emissions For 1.187 Joules of Additional Energy Over Stock

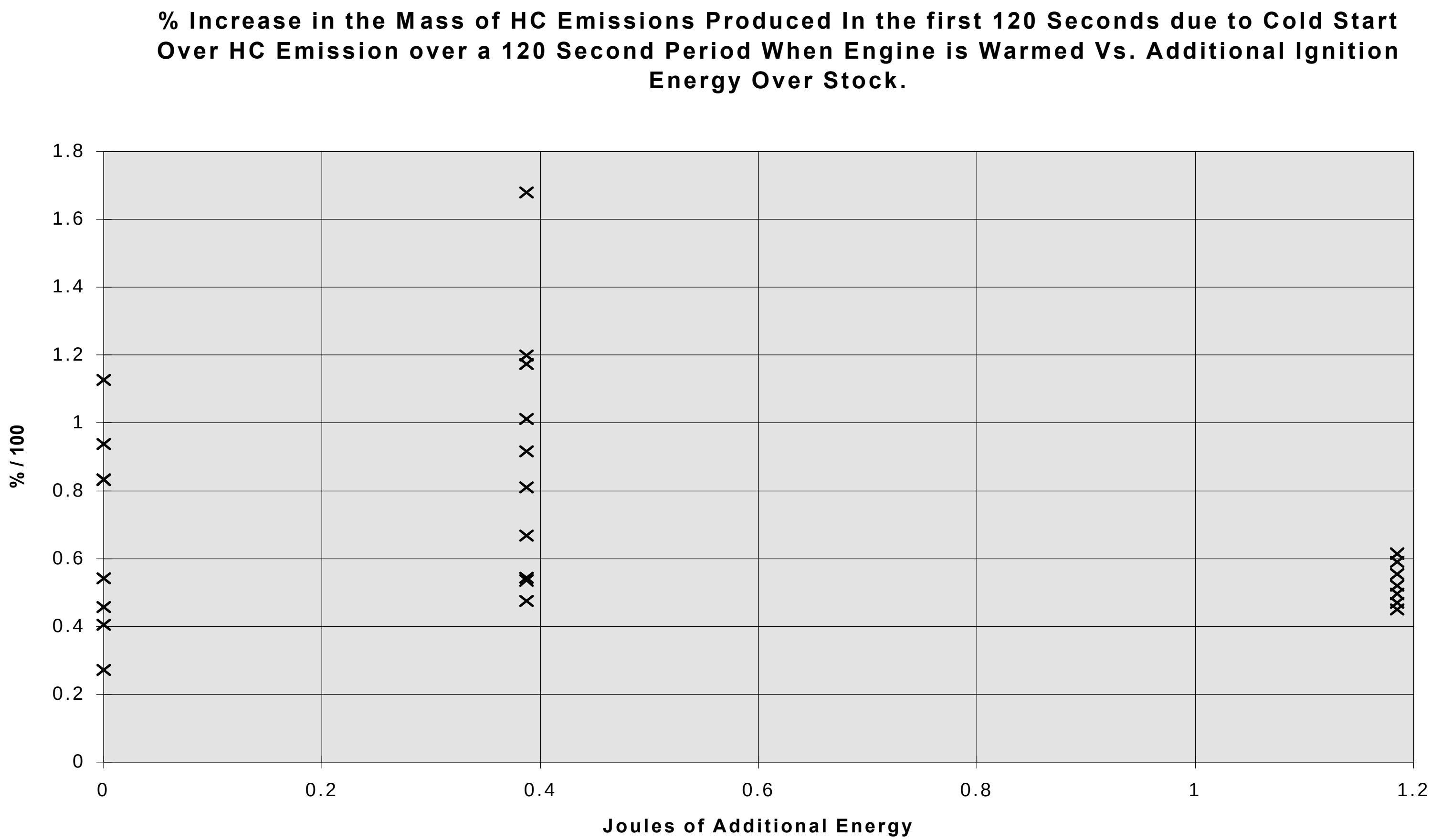

Figure 4.7 - % Increase in Contribution to Total HCs Produced by Cold Start Vs. Additional Ignition Energy Over Stock

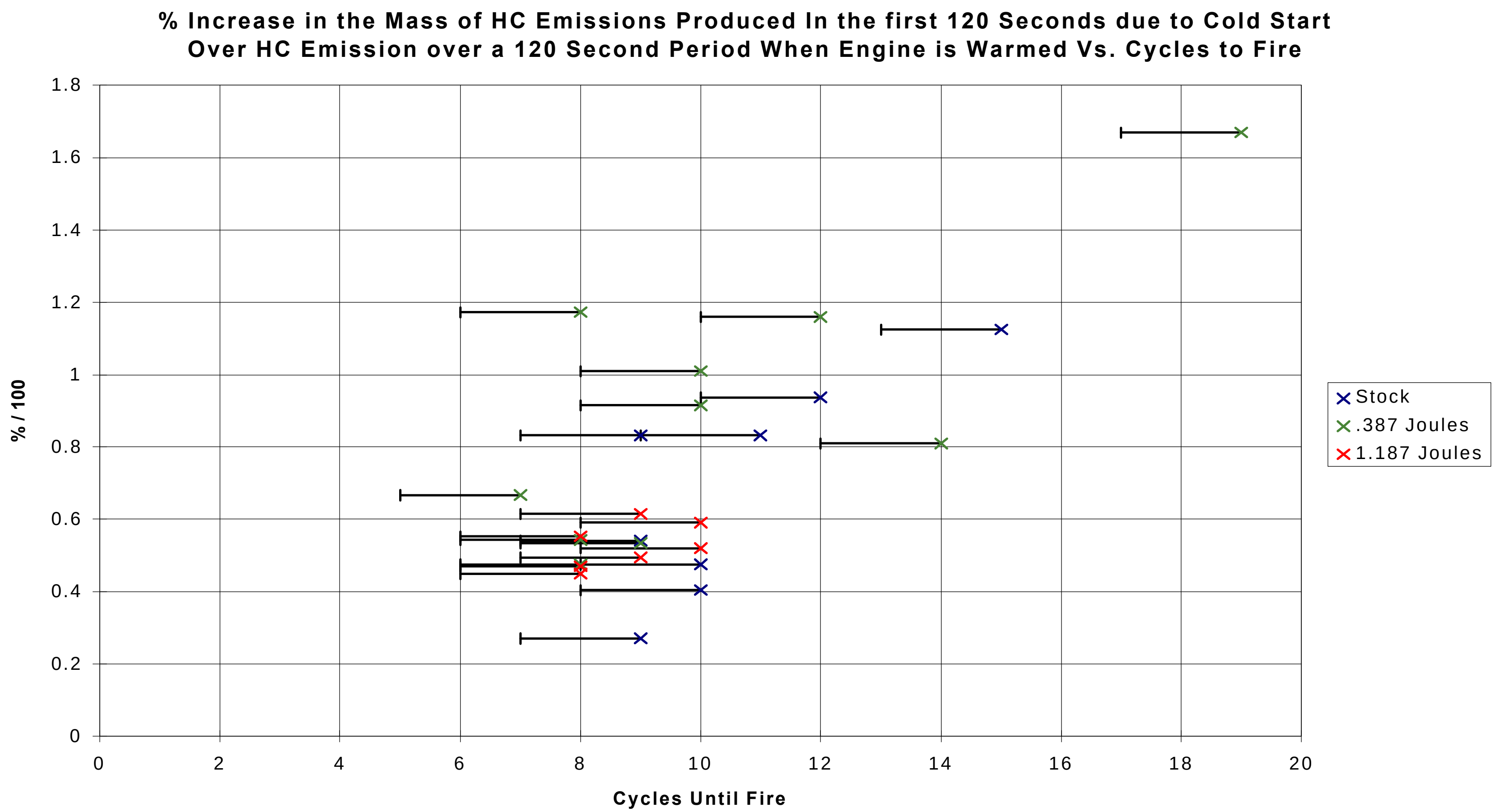

Figure 4.8 - % Increase in Contribution to Total HCs Produced by Cold Start Vs. Cycles Until Start

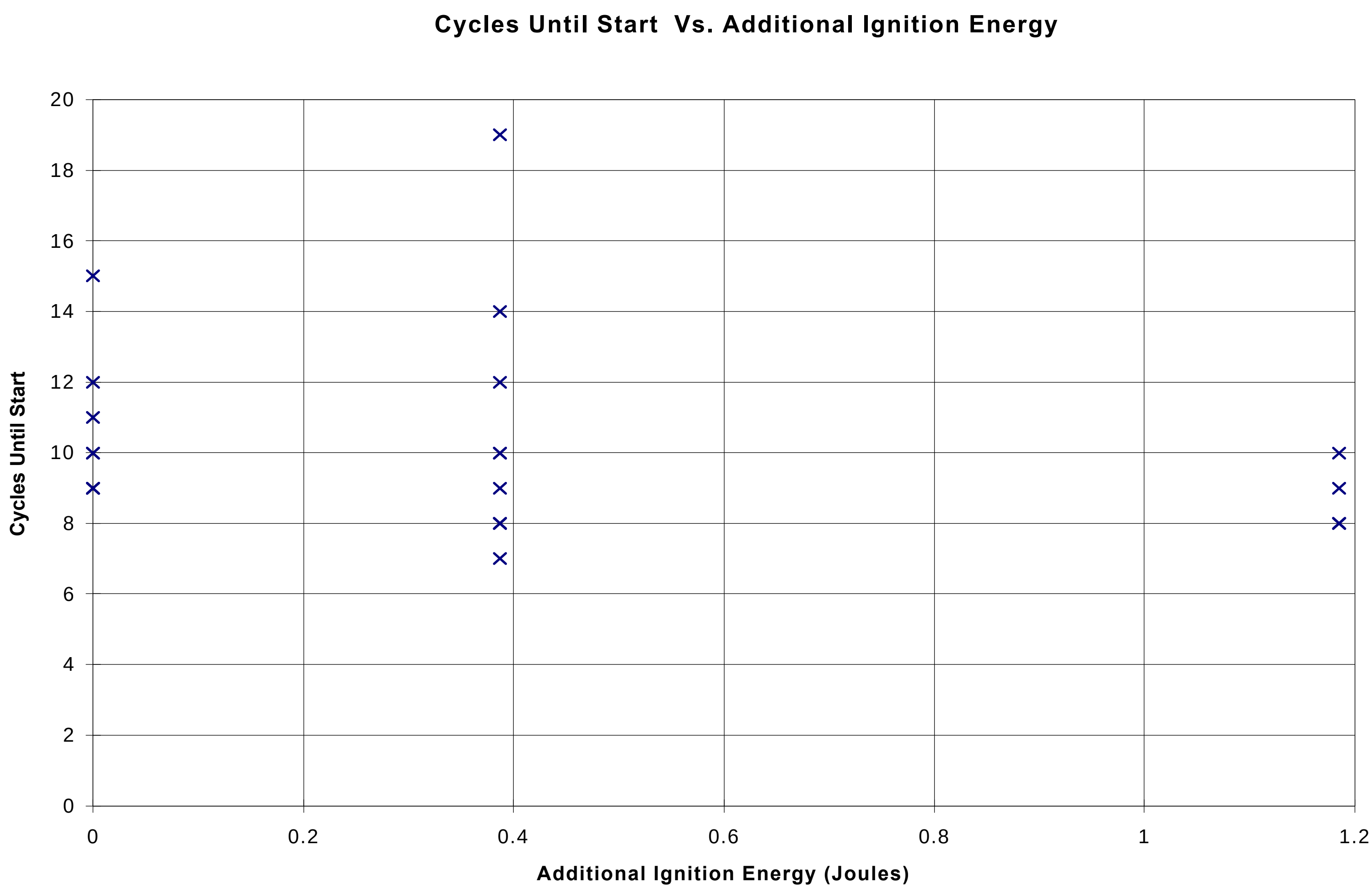

Figure 4.9 - Number of Cycles Until Start for the Three Energy Levels

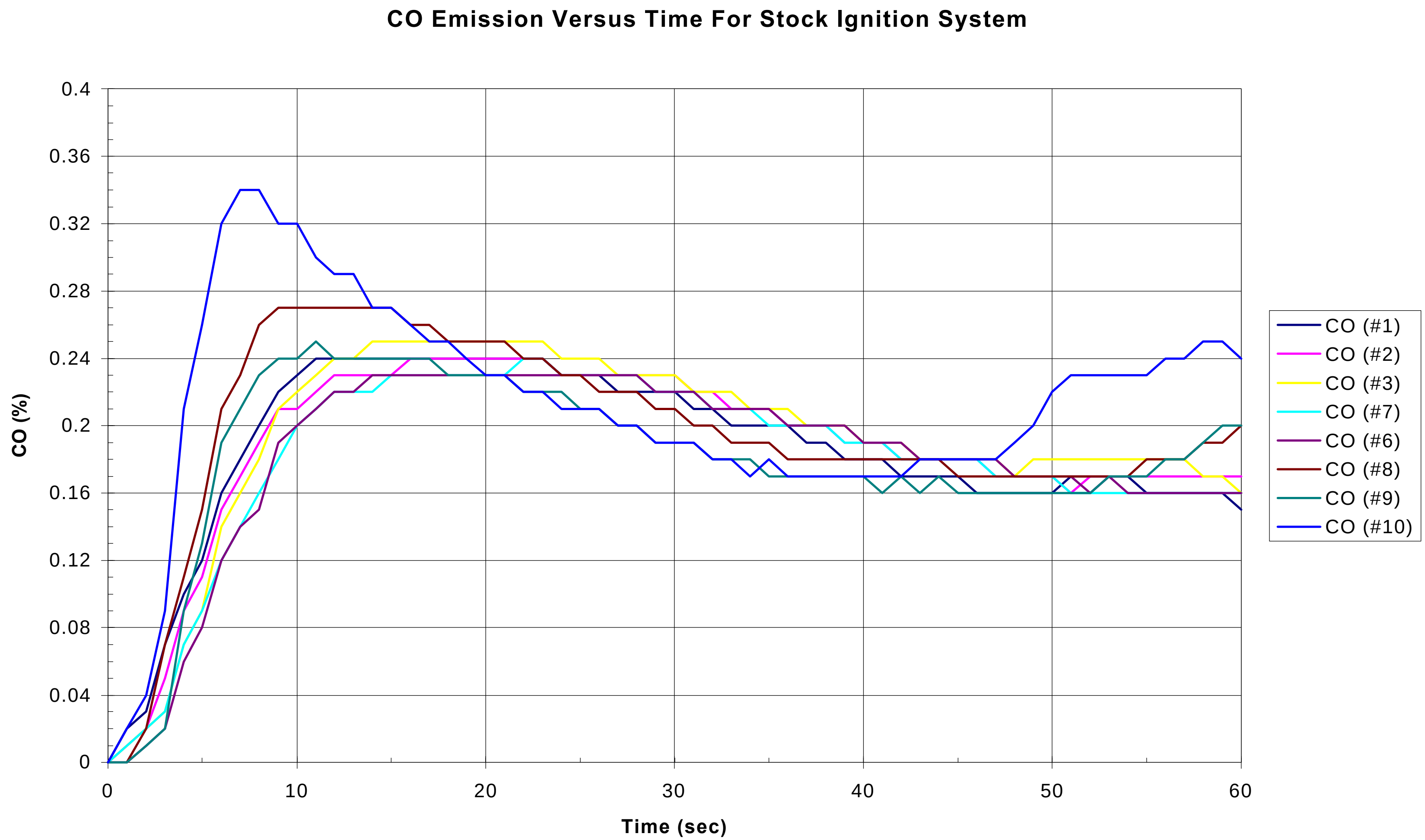

Figure 4.10 - CO Emission for Stock Ignition System

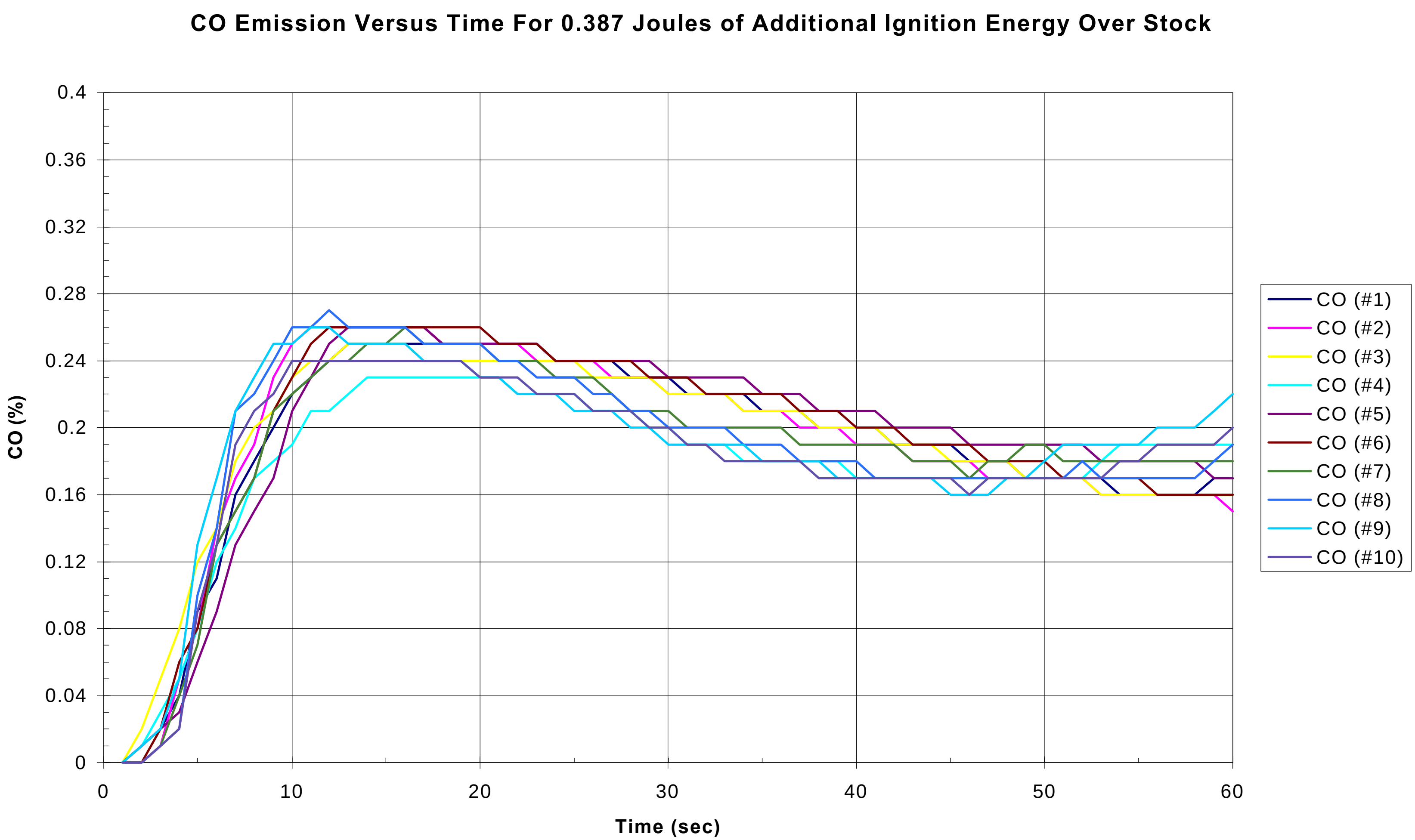

Figure 4.11 - CO Emissions For 0.387 Joules of Additional Energy Over Stock

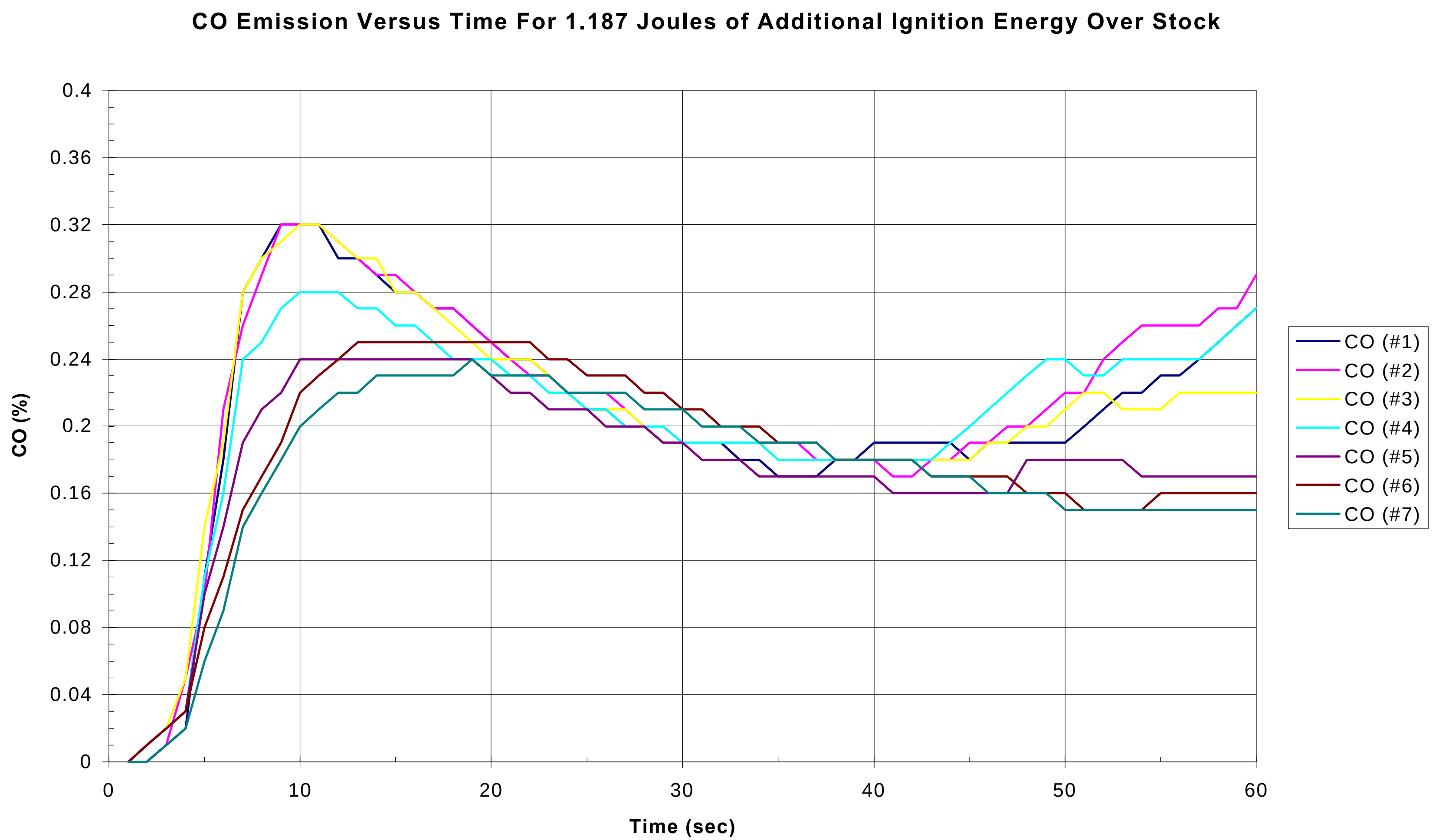

Figure 4.12 - CO Emissions For 1.187 Joules of Additional Energy Over Stock

4.2 Discussion

4.2.1 Effects on Emissions

From the results obtained during the series of tests, increasing the energy supplied for ignition appeared to have an effect on the cold start nature of the test engine. Increasing the ignition energy showed changes in the amount of HC and CO produced after initial startup of the engine. The increased ignition energy also demonstrated the ability to reduce the variations in the time after the first fuel was injected until the engine started.

The HC emission measured during the experiment trace out a typical HC concentration versus time curve for the cold start of an engine. The curve is characterized by a sharp peak at the beginning that levels out within about a minute. The large amount of excess fuel provided during the engine's initial cranking and over the first few seconds of a operation create the peak. After the engine starts and warms up, some the enrichment is reduced thus the HC curve levels out at a substantially lower concentration. The amount of enrichment and the length depends on the ability of the supplied fuel to form enough vapor to support combustion.

Comparing HC emissions data, the highest level of additional ignition energy demonstrated a clear ability to reduce HC emissions and provide consistent start times. The highest ignition energy level had 1.187 joules of additional energy supplied to the spark plug. At this level, the ignition system reduced the average HC peak emission by around 121 ppm or 14% over the stock ignition system and reduced the standard deviation of the sample by half (Table 4.1,4.3). The 0.387 joules additional energy level performance was hard to evaluate when compared to the stock ignition's performance. Its performance appeared about equal to the stock given when the average peak HC emissions and the % cold start HC contribution data in Figure 4.8. A closer look at the raw data plotted in Figure 4.3, the data shows a decrease in HC production. In this graph, the majority of the HC peaks fall under and around 800 ppm. The stock ignition's raw HC data (Figure 4.1) shows the majority of its HC peaks range from 810 ppm and up. The normalized graphs gives no information to support either case (Figure 4.2,4.4). Both graphs show the same amount of scatter. The raw data suggest that there is a

Increased ignition energy showed the most effect on cold start at the highest setting. At this setting, 1.187 joules of additional energy, the results became more pronounced. Better result might be obtained if more ignition energy was added past this point. At 0.387 joules of additional energy, the effects of the stock ignition on the initial arc formation could have had a larger impacted the total arc formation thus affecting the overall performance. The high energy ignition system was capable of providing energy up to 2.4 joules. However, at levels higher than what was used during testing, the high energy ignition held a constant arc across the spark plug. Increasing the gap would decrease the ability for the constant arc to form. However, increasing the spark plug gap would have a negative impact on the ability of the stock ignition to from the initial breakdown allowing the high energy system to discharge. Deteriorating the performance of the stock ignition hurts the high energy system. Combining the two system to form one variable energy ignition system would make a better design. This would eliminate the weak link in the chain, the stock ignition.

HC emissions from the experiment were linked to number of cycles before the first fire also. An appreciable increase in these pre-start cycles resulted in an increase in the peak HC levels. The test engine in this experiment started between 8 and 12 cycles on average. For a new modern production vehicle with optimized fuel injection programming, 8-12 cycles is excessive, so the amount of engine cranking HC emissions emitted would be lower. However, as cars increase in age and mileage, the number of cranking cycles needed to start increases as due emissions. On a car with 100,000 miles 8-12 cranking cycles appears less excessive. With the durability regulations on emissions controls becoming more strict, maintaining a low number of cranking cycles during start up in older vehicles increases in importance. Increased ignition energy may be a way assist aging vehicles.

Results of the increased ignition energy on the formation of CO during the cold start compliments the HC emissions. With the small decreases in the HC produced, the CO concentration was expected to rise slightly. In Figure 4.8 - 4.10, small increases in the amount of CO are observed. Because the largest change in the average HC over the range of ignition energies was only on the order of 100 ppm, the changes in the concentration of CO remain close to the uncertainty limits of the CO analyzer at .05%. The start-up emission's peak in CO occurs at the same time as the peak in HC occurring with in the first 20 seconds. Comparing the CO results between the stock ignition and 0.387 joules (Figure 4.8, 4.9), more support is formed to argue that even at 0.387 joules of additional energy the energy increase affects the quality of combustion. The graphs show that the 0.387 joule increases the CO concentration increases by .01-.02%. The concentrations of the CO rose from 0.24% -0.25% up to 0.25%-0.26% . To more accurately determine the changes in CO at this level a more accurate CO analyzer is needed.

4.2.2 Test Apparatus Discussion

Assessing the data recorded during the test gave insight into previously unknown conditions taking place within the experimental setup and into ways to redesign the experimental setup to provide a more accurate study of cold start emissions. The data showed unexpected trends at every ignition energy level in the emission concentrations. Because the trends were consistent through the three energy levels, their causes were linked to the experimental setup and procedure. Most of the trends are explained.

Figure 4.12 shows a typical trace of the emissions and data trends recorded over the 12 minutes run of the test. While the first 2 minutes were of interest in the study of cold start, looking at the trends in the data during the warmed operation provided useful setup information. Warmed engine emissions are more predictable then cold start emissions. The changes from predicted values are easier to spot and explain in this range of operation. The fluctuations in the values past 150 seconds stand out in the data. An example of the typical fluctuations are shown in Figure 4.12. All the curves fluctuated at the same time. This synchronization in the fluctuation pointed to a common root cause. The root cause in the fluctuation was determined to be fluctuations in the supplied A/F ratio. In designing the setup it was assumed that the air flow into the engine was constant because the air was supplied at constant temperature and pressure with the engine operating at a constant speed. Under this constant air flow assumption the fuel injector was programmed to inject at a rate that would create the desired A/F ratio. After 60 seconds the injectors were programmed to supply enough fuel for an A/F ratio of 14.7. After collecting the emissions concentrations and calculating the operating A/F ratio, it was clear that the actual A/F ratio was not always what was intended.

Figure 4.13 shows a typical temperature versus time trace and its relationship to the calculated A/F ratio. The graph shows a strong connection between the two. During the test, the engine was allowed to heat up to 90° C then the coolant water was turned on and off to maintain temperatures around 90° C. The sudden flow of cold water around the engines cylinder wall cooled the cylinder wall enough to create a significant increase in volumetric efficiency. The increase in volumetric efficiency made the engine run lean. This effect can be seen in Figure 4.13. The engine cycles from rich to lean as the cylinder wall temperature goes from hot to cold. The effects of wall temperature on the A/F ratio and the exhaust products are shown in Figure 4.12. When the A/F goes rich (the blue line dips under the red line) or lean the concentration distribution of the measured exhaust products react accordingly.

The CO concentration increased when the mixture became richer. CO_2, O_2, and the NO_x concentrations fell. The level of HC emitted also shows a slight increase with the richer mixture. The general trend induced in the CO concentration by the fluctuation of the A/F ratio was validated using STANJAN to model the chemical equilibrium concentrations. Figure 4.14 has the STANJAN results and the measured results for comparison of the general trend. A range of A/F ratios calculated from the exhaust products were entered in to STANJAN. The A/F ratios were taken from the 224 to 267 second range in run #6 for the 1.187 joules of additional energy test. Given the reactants, the most common products, and estimate of the conditions, the program calculated the equilibrium concentrations. The actual values of the concentrations varied because the program model for the molecular balance was simplified. For the STANJAN calculation, Iso-octane (C_8H_{18}) was used as the fuel.

The variation of actual A/F ratio from the expected value also appeared in the cold start phase (the 2 minutes). The short peak in CO concentration followed by a decrease in the concentration then another rise was cause for further investigation. The reason for the strange CO behavior was again A/F changes. The pulsewidth for the fuel injector was programmed to be 30 ms for the first 3 seconds then ramp down to 21.2 ms in a straight line over the next 57 seconds. The pulsewidth of 21.2 ms was determined to create an A/F 14.7 while the engine was at operating temperature. The 30 ms was determined to be the pulsewidth needed to start the engine when at 18° C and produce an A/F ratio of 10.5 when the engine was at operating temperature. The combination of the pulsewidth decreasing and the increased volumetric efficiency during the first minute of operation caused the actual supplied A/F ratio to go lean within the first 50 seconds. The leaning of the mixture caused the decrease in the CO level after the initial start up. Figure 4.15 shows a sample of the measured A/F ratio versus time and the A/F ratio estimated to be actually supplied after correcting the computer programmed A/F curve for the changes in temperature and volumetric efficiency with time. The correction is a rough estimation based on the effects of the changing volumetric efficiency on the A/F ratio over the 60 to 120 second range. Since the fuel injected per cycle after 60 was constant, any changes in A/F were due to the changing air charge.

The unplanned sudden leaning out of the mixture was advantageous in studying the cold start process. The faster the mixture is leaned out after the first successful combustion cycle the more pronounced the effects of the excess fuel needed to produce that first successful cycle are. The longer the mixture stays unnecessarily rich the more blurred the initial level of emission become.

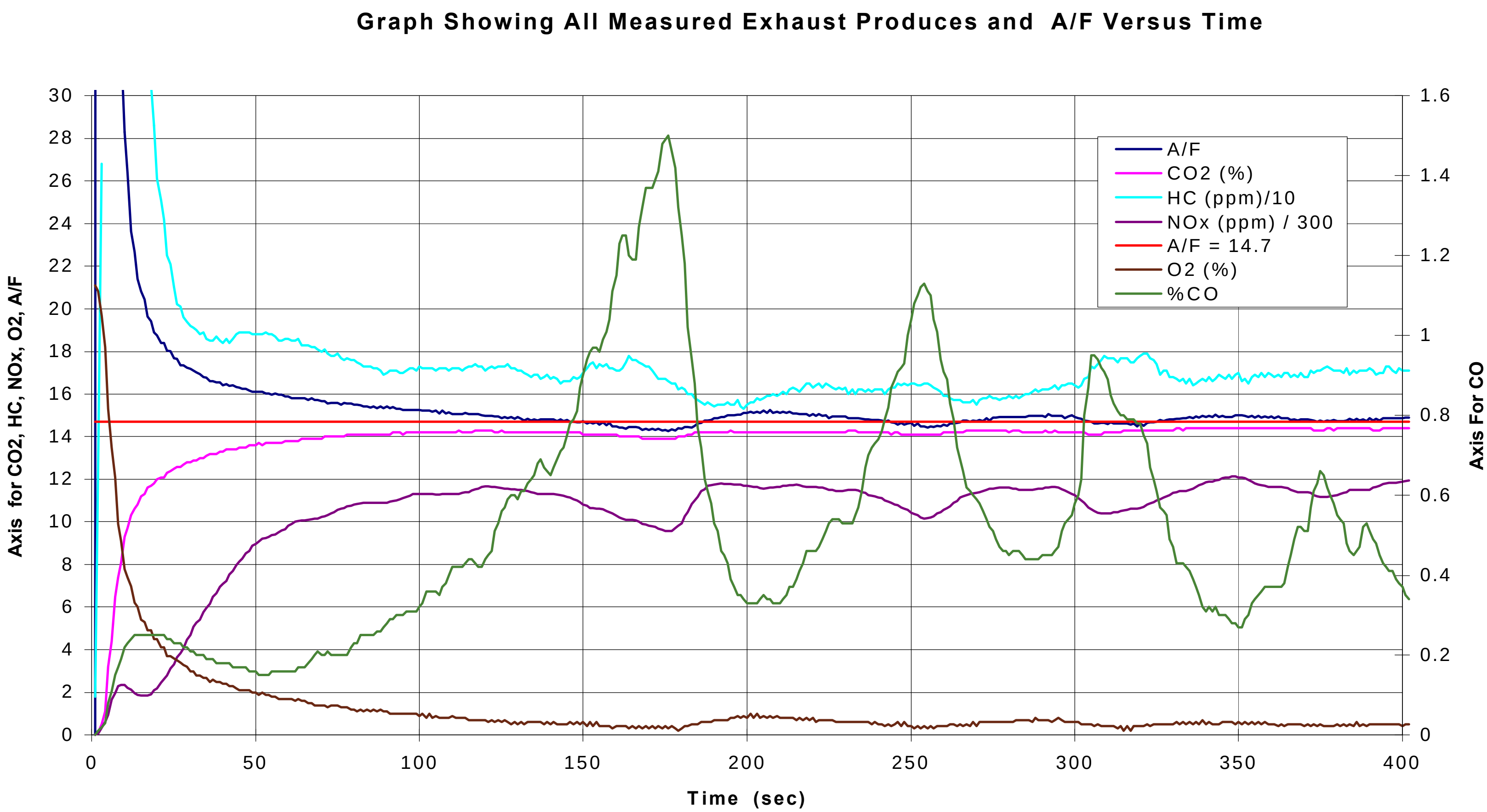

Figure 4.12 - Example Graph of All the Measured Emissions and Calculated A/F Ratio Versus Time

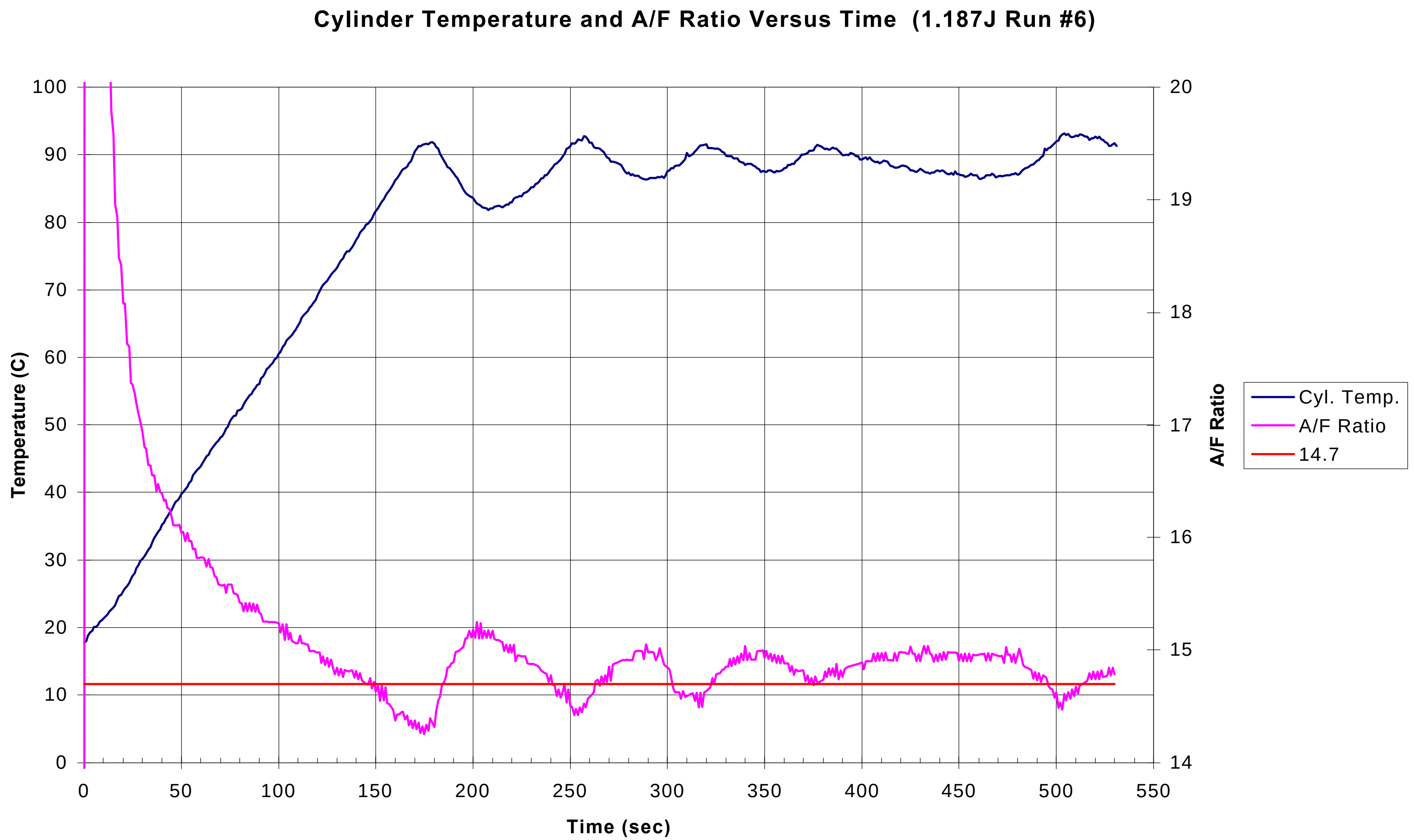

Figure 4.13 - Cylinder Temperature and Calculated A/F Ratio Versus Time

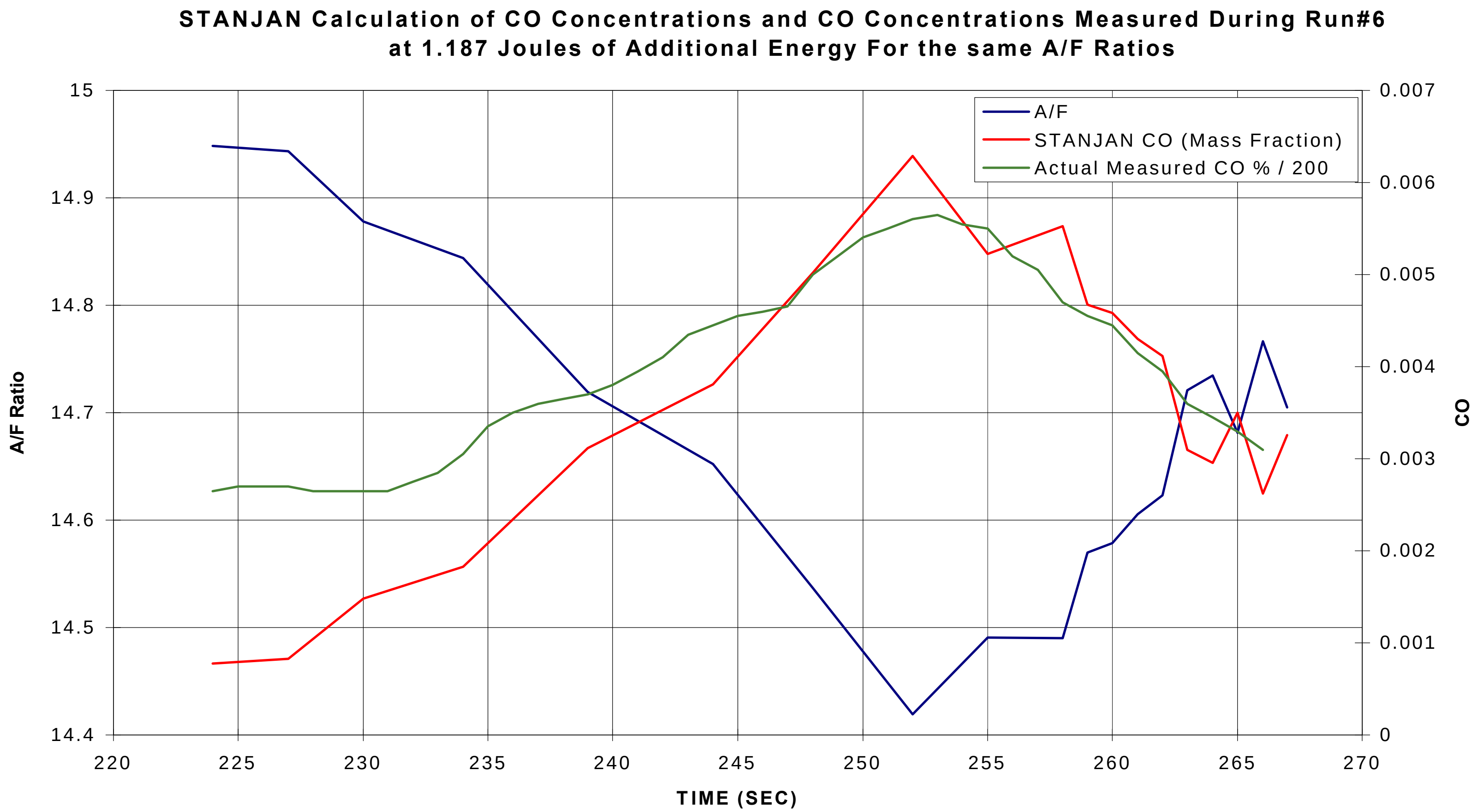

Figure 4.14 - Comparison of Estimated CO Concentration Changes and Measured CO Concentration Changes For A/F Ratio Fluctuations

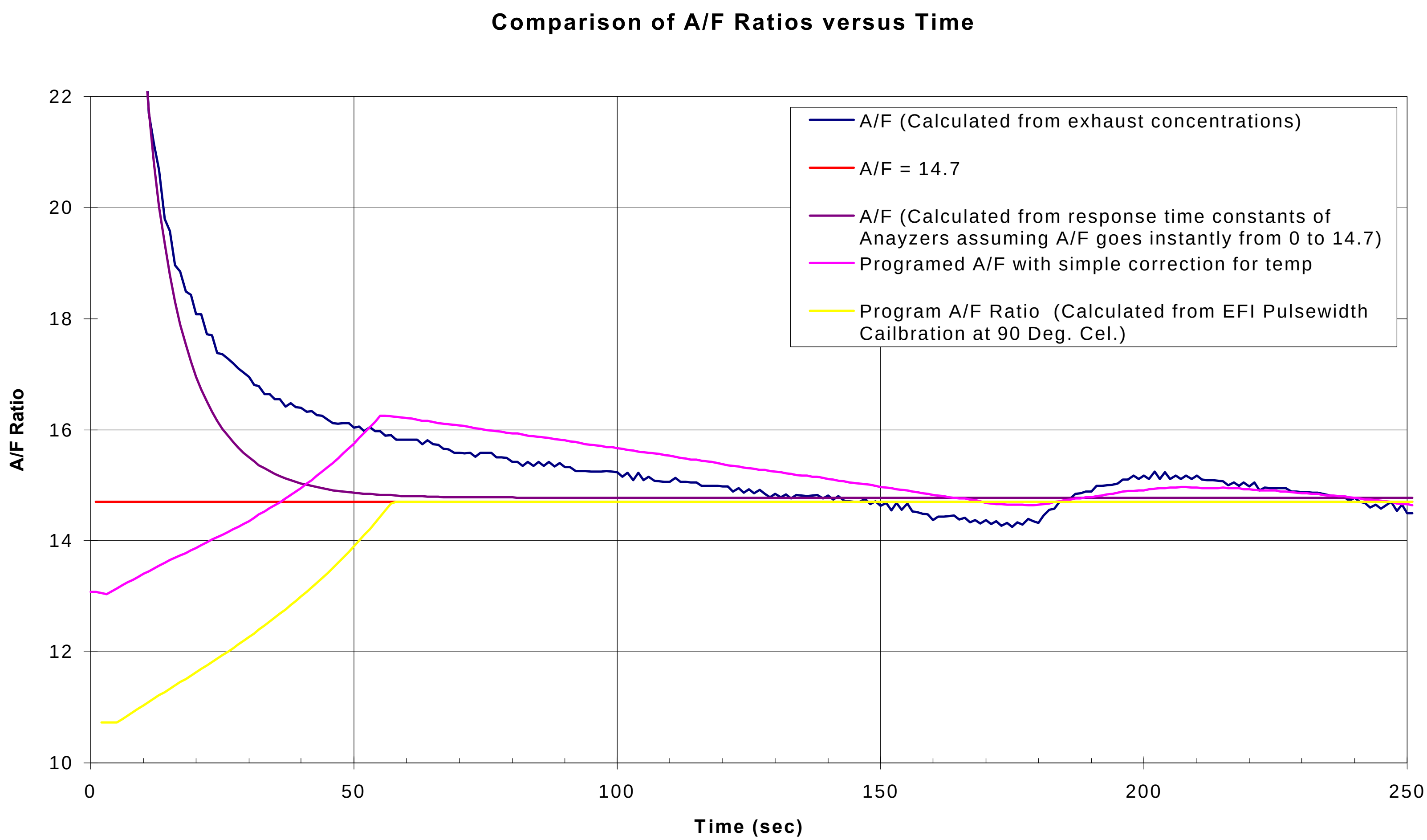

Figure 4.15 - A/F Ratio Comparison Graph